A miniaturized passive sampling-based workflow for monitoring chemicals of emerging concern in water

Alexandra K. Richardson [a,e], Rachel C. Irlam [b], Helena Rapp Wright [e], Graham A. Mills [c], Gary R. Fones [c], Stephen R. Stürzenbaum [a], David A. Cowan [a], David J. Neep [d], Leon P. Barron [e,*]

[a] Dept. Analytical, Environmental & Forensic Sciences, Institute of Pharmaceutical Sciences, School of Cancer and Pharmaceutical Sciences, Faculty of Life Sciences & Medicine, King's College London, 150 Stamford Street, London SE1 9NH, United Kingdom
[b] Dept. Chemistry, School of Natural and Environmental Sciences, Newcastle University, Newcastle-upon-Tyne, NE1 7RU, United Kingdom
[c] Faculty of Science and Health, University of Portsmouth, White Swan Road, Portsmouth PO1 2DT, United Kingdom
[d] Agilent Technologies UK Ltd, Essex Road, Church Stretton SY6 6AX, United Kingdom
[e] Environmental Research Group, MRC Centre for Environment & Health, School of Public Health, Faculty of Medicine, Imperial College London, 86 Wood Lane, London W12 0BZ, United Kingdom

HIGHLIGHTS

- Miniature 3D-printed passive sampler devices (3D-PSD) enabled scaled down workflow.
- Uptake rates (R_s) determined for 39 contaminants of emerging concern (CECs)
- R_s smaller on 3D-PSDs and more sensitive LC-MS methods required
- Agreement between PSD-extrapolated CEC concentrations and those measured in water.
- 80 CECs detected and a further 113 tentatively identified in river 3D-PSD extracts.

GRAPHICAL ABSTRACT
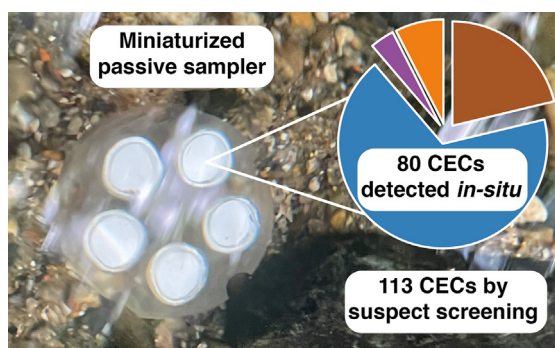
ARTICLE INFO

Editor: Damia Barcelo

ABSTRACT

The miniaturization of a full workflow for identification and monitoring of contaminants of emerging concern (CECs) is presented. Firstly, successful development of a low-cost small 3D-printed passive sampler device (3D-PSD), based on a two-piece methacrylate housing that held up to five separate 9 mm disk sorbents, is discussed. Secondly, a highly sensitive liquid chromatography-tandem mass spectrometry (LC-MS/MS) method reduced the need for large scale in-laboratory apparatus, solvent, reagents and reference material quantities for in-laboratory passive sampler device (PSD) calibration and extraction. Using hydrophilic-lipophilic balanced sorbents, sampling rates (R_s) were determined after a low 50 ng L^{-1} exposure over seven days for 39 pesticides, pharmaceuticals, drug metabolites and illicit drugs over the range 0.3 to 12.3 mL day^{-1}. The high sensitivity LC-MS/MS method enabled rapid analysis of river water using only 10 μL of directly injected sample filtrate to measure occurrence of 164 CECs and sources along 19 sites on the River Wandle, (London, UK). The new 3D-PSD was then field-tested over seven days at the site with the highest number and concentration of CECs, which was down-river from a wastewater treatment plant. Almost double the number of CECs were identified in 3D-PSD extracts across sites in comparison to water samples (80 versus 42 CECs, respectively). Time-weighted average CEC concentrations ranged from 8.2 to 845 ng L^{-1}, which were generally comparable to measured concentrations in grab samples. Lastly, high resolution mass spectrometry-based suspect screening of 3D-PSD extracts enabled 113 additional compounds to be tentatively identified via library matching, many of which are currently or are under consideration for the EU Watch List. This miniaturized workflow represents a new, cost-

* Corresponding author.
E-mail address: leon.barron@imperial.ac.uk (L.P. Barron).

effective, and more practically efficient means to perform passive sampling chemical monitoring at a large scale.

Synopsis: Miniaturized, low cost, multi-disk passive samplers enabled more efficient multi-residue chemical contaminant characterization, potentially for large-scale monitoring programs.

1. Introduction

Chemical contamination of the aquatic environment from anthropogenic sources is well reported and is of growing concern as knowledge of the long-term effects in the environment evolves. Upwards of 630 chemicals, including pharmaceuticals, personal care products, and pesticides have been identified in 71 countries worldwide, often in multiple environmental compartments (aus der Beek et al., 2016; Zenker et al., 2014; Noguera-Oviedo and Aga, 2016; Patel et al., 2019; Wang et al., 2020). However, over 350,000 chemicals are currently licensed for manufacture and sale globally making this an enormous analytical challenge (Wilkinson et al., 2018). Some of these, including pesticides, pharmaceuticals, and personal care products, are classified as contaminants of emerging concern (CECs) in Europe according to the EU Water Framework Directive and the Marine Strategy Framework Directive (European Commission, 2015; European Commission, 2018; EC, 2008; European Commission, 2013). Similarly, many are listed on the United States Environmental Protection Agency's most recent Contaminant Candidate List (CCL4) (US Enviromental Protection Agency, 2021).

Various methods exist for the spatiotemporal monitoring of CECs in the aquatic environment and passive sampling is now being increasingly used. Passive sampling devices (PSDs) have been suggested as a viable monitoring approach within the EU Water Framework Directive (Brack et al., 2017). Several qualities make it an appealing alternative to grab or composite sampling. First is the ability to calculate a time-weighted average (TWA) concentration of CECs over extended periods in the case of integrative PSDs (Caban et al., 2021). For this, a compound-specific sampling rate (R_s) is determined either in the laboratory or in the field (Taylor et al., 2020; Vrana et al., 2021; Townsend et al., 2018). PSDs can offer greater sensitivity compared to grab sampling, as the accumulated compounds are often enriched on the sorbent in situ (Becker et al., 2021). One drawback is that the TWA concentration obtained from PSDs fails to reflect short pulsed pollution events. However such events are often missed entirely when using grab sampling. Many PSD formats exist, depending on the application (Taylor et al., 2020; Namieśnik et al., 2005; Taylor et al., 2019). For the measurement of CECs in the aquatic environment, the most common PSDs are the Chemcatcher®, the polar organic chemical integrative sampler (POCIS) devices and diffusive gradient in thin-films (o-DGT) devices (Taylor et al., 2020). The Chemcatcher® holds standard 47 mm SPE sorbent disks (Charriau et al., 2016). POCIS devices contain free sorbent particles held between two porous membranes, again of similar diameter (Alvarez et al., 2004). The Chemcatcher® is limited to one size containing one disk per device, making multimodal and replicate deployments cumbersome, especially when several passive samplers are required and the sampling location is not easily accessible. Tailored and often large equipment is regularly required to perform R_s CEC calibrations in the laboratory, in addition to often relatively expensive quantities of reference materials for large volume exposures (Charriau et al., 2016). Specifically, to enable calculation of R_s, preconcentration of up to 1 L of water is often required for each measurement to be made robustly at the ng L^{-1} level necessitating the use of large exposure volumes when calibrants across multiple timepoints are required (Grodtke et al., 2020). Recent advances in liquid chromatography-mass spectrometry (LC-MS) technologies have resulted in methods that can now detect CEC concentrations at this level using direct injection of a filtered sample (Richardson et al., 2021; Hermes et al., 2018; Boix et al., 2015; Ng et al., 2020). In addition, for extraction of 47 mm diameter PSDs themselves, frequently 40 mL of organic solvents are used which can amount to sizeable total volumes used for large monitoring campaigns, even when in situ R_s calibrations are employed (Petrie et al., 2016).

Therefore, an opportunity exists now not only to scale down the entire passive sampling process, including PSDs to match analytical sensitivity gains, but also any associated apparatus and chemical reagents required for calibration to potentially make passive sampling more accessible and sustainable for analytical laboratories.

The increased affordability and resolution of modern benchtop 3D-printers makes them very useful for prototyping. Compared to traditional manufacturing techniques, 3D-printing can accurately produce unique, identical objects without the need for tooling or fabricating master molds, whilst generating minimal waste (Gross et al., 2017; Kalsoom et al., 2018a). Its flexibility has resulted in it being applied in several different scientific disciplines, ranging from microfluidics to medicine and biology (Chan et al., 2015; Villegas et al., 2018; Yuen, 2016; Anderson et al., 2013; Chen et al., 2014; Yuen, 2008). For passive sampling, only two relevant studies exist utilizing 3D-printing (Kalsoom et al., 2018b; Nitti et al., 2018). Kalsoom et al. used multi-material fused deposition modelling (MM-FDM) to build a low-cost, membrane-integrated PSD housing for the uptake of atrazine. Here, a polylactic acid filament was used for the sampler housing and a composite Poro-Lay Lay-Felt filament produced the integrated membrane. It was functionally similar to POCIS, using polystyrene SPE sorbent particles (Kalsoom et al., 2018b). Nitti et al. employed FDM 3D-printing to create a flow-through attachment for an existing polymer inclusion membrane (PIM)-based PSD that shielded the device from environmental fluctuations in flow targeting zinc(II) (Nitti et al., 2018; Almeida et al., 2016). However, knowledge regarding the wider applicability of 3D-printed devices for more and chemically diverse compounds is critically lacking, especially where they could be used for large-scale monitoring programs.

The aim of this work was to scale down an entire workflow for passive sampling and analysis of CECs in river water. To achieve this aim: (a) prototype PSD designs capable of holding multiple smaller fiberglass-particle composite-type sorbent disks were developed and characterised; (b) a scaled-down calibration experiment on a hydrophilic-lipophilic balanced (HLB) sorbent was performed at low CEC exposure concentrations using a highly sensitive LC-MS/MS method which was capable of performing direct injection analysis of water at the ng L^{-1} concentration level; and (c) the 3D-PSDs were field-tested in the River Wandle (London, UK) for targeted CEC monitoring, and a comparison to measured CEC concentrations made in water directly, and (d) the potential for suspect screening of 3D-PSD extracts to identify additional CECs, as well as their metabolites and transformation products, was assessed. This work presents the first investigation of a low-cost miniaturized, integrated, and multiplexed 3D-PSD for multi-residue CEC monitoring in environmental waters.

2. Materials and methods

2.1. Analytical and experimental reagents

All reagents used were of analytical grade or higher unless stated otherwise. Methanol (MeOH), acetonitrile (MeCN), and propan-2-ol (IPA) were sourced from Sigma-Aldrich (Gillingham, Dorset, UK) and LC-MS grade formic acid was purchased from Millipore (Millipore, Bedford, USA). A standard mix of 200 compounds (n = 164 analytical standards and n = 36 stable isotope-labelled internal standards (SIL-IS), purity ≥97%) was used throughout this study for both quantitative and/or qualitative purposes and full details are listed in the electronic supplementary information, Table S1.

Salts for the preparation of artificial freshwater (AFW) included magnesium sulfate ($MgSO_4$) (Fisher Scientific, Leicestershire, UK), sodium hydrogen carbonate ($NaHCO_3$) and potassium chloride (KCl) (both from Alfa Aesar, Massachusetts, USA), and calcium chloride ($CaCl_2$) (ACROS Organics, Geel, Belgium). AFW was prepared as per the OECD Test Guideline No.203 by diluting stock solutions of $CaCl_2$, $MgSO_4$, $NaHCO_3$, and KCl to 2.0 mM, 0.50 mM, 0.77 mM, and 0.07 mM, respectively with ultrapure water dispensed from an 18.2 MΩ.cm Millipore Milli-Q water purification system (MilliporeSigma, Massachusetts, USA) (OECD, 2019).

2.2. Instrumental analysis

LC-MS/MS was performed using an LCMS-8060 (Shimadzu Corporation, Kyoto, Japan) according to Ng et al. and Richardson et al (Richardson et al., 2021; Ng et al., 2020). Separations were performed using a Raptor 5.0 × 3.0 mm, 2.7 µm biphenyl guard column (Restek, Pennsylvania, USA). The injection volume was 10 µL for all samples and the flow rate was 0.5 mL min^{-1}. A binary LC gradient consisted of 0.1% *v*/v aqueous formic acid as mobile phase A and 0.1% v/v formic acid in 50:50 MeOH:MeCN as mobile phase B. The elution program included an initial hold of 10% B for 0.2 min, a linear ramp to 60% B over 2.8 min, and a 100% B hold for 1 min. The total run time was 5.5 min, including a 1.5 min re-equilibration time. Compounds were identified from a minimum of two transitions per compound where possible using multiple reaction monitoring (MRM) with a varying dwell time between 1 and 20 ms (analyte dependent). All data were acquired and processed using Shimadzu LabSolutions and LabSolutions Insights LCMS software v3.7, respectively.

Suspect screening was performed on a Shimadzu LCMS-9030 LC-QTOF-MS system. Separations were performed using a Shim-pack Velox 2.1 × 100 mm, 2.7 µm biphenyl column (Shimadzu) held at 40 °C with a 17-min binary gradient elution program. The flow rate was 0.3 mL min^{-1} with a 40 µL injection volume of 3D-PSD extracts in both positive and negative electrospray ionization (ESI) mode. Mobile phases were 2 mM ammonium formate with 0.002% formic acid in either ultrapure water or methanol (Mobile Phases C and D, respectively). The program consisted of 5% D for 1 min, followed by a quick ramp to 40% D over 2 min, and then ramped to 100% D to 10.5 min. At 11.01 min the analytical run ended and the post-run column clean-up/re-equilibration program was initiated. The flow rate was then increased to 0.5 mL min^{-1}, still at 100% D for 2 min. At 13.01 min re-equilibration to initial mobile phase conditions was then performed at the elevated flow rate. Finally, flow rate was returned to 0.3 mL min^{-1} at 14.01 min for the remainder of the run at 17.0 min. The initial MS scan range was 100–920 Da for positive 50–920 for negative mode. Data independent analysis (DIA) fragmentation with variable isolation width and a collision energy of 30 ± 25 and 25 ± 15 V was used for positive and negative mode, respectively with a scan time of 25 and 28 ms, respectively. Fragments were monitored for between 40–920 and 50–920 Da for positive and negative mode, respectively.

Retrospective suspect screening was performed in LabSolutions Insight Explorer Library Screening software v3.8 SP1 against a list of $n = 1219$ compounds which included the Shimadzu toxicology screening library, Shimadzu pesticide library and additional reference materials data from Imperial College London. All 3D-PSD extracts were searched against this list and candidates shortlisted based on four points of confirmation. These included retention time (RT) within 0.5 min of the curated library value, mass accuracy within 5 ppm, isotopic distribution score >20 and a library identification similarity index score >45. In addition, the signal-to-noise ratio was greater than 3:1 and peak intensity greater than 1000 for all shortlisted candidates.

2.3. Design and fabrication of the 3D-printed PSD

All 3D-printed parts were fabricated using a SLA-based Asiga MAX mini 3D printer (Puretone™ Ltd., Kent, UK) and a methacrylate-based resin (PlasCLEAR V2). This printer was suitable for the required resolution and PlasCLEAR was stable across acidic-alkaline pH and in a range of organo-

aqueous solvents typically used for water sample preparation (Irlam et al., 2020). Computer-aided designs (CAD) were developed, produced, and exported as *.STL files using the Solid-Works software (Dassault Systems, Waltham, MA, USA). The files were sliced and uploaded to the 3D printer via the Asiga Composer application (Asiga, Anaheim Hills, CA, USA). All parts were printed with a layer thickness of 50 µm, a light intensity of 30.4 mW cm^{-2}, and an exposure time of 2.34 s. See SI for all build conditions and final *.STL files (Table S2). The total print time was 1.93 h and the cost of the housing material per device was £2.37 in Great British Pounds (GBP) including a transport cap (Fig. 1 (b) – (d)). All parts were washed twice by sonication (15 min) in IPA to remove excess resin. Parts were air dried before an additional 30-min cure under UV light using the Asiga Flash UV oven (Puretone™ Ltd., Kent, UK). All parts were stored dry and were rinsed with MeOH and water before use.

2.4. Characteristics of 3D-PSDs

Physical characteristics of the cured resin were assessed with scanning electron microscopy (SEM) using a JSM-IT100 (JEOL, Akishima, Tokyo, Japan). For imaging, 1 mm^3 and 0.5 mm^3 cubes were printed using the same build conditions as the 3D-PSD and prepared for imaging by first being mounted on aluminium stubs with self-adhesive carbon tape before sputtering with gold under argon (Automatic Sputter Coater, Agar Scientific, Essex, UK). Print porosity was determined via the Brunauer–Emmett–Teller (BET) method using a TriStar II instrument (Micromeritics, Norcross, USA). Samples were degassed overnight at ambient temperature with nitrogen before analysis. A sub-set of 136 physicochemically diverse CECs that could be quantified reliably at low ng L^{-1} concentrations were used to assess sorption to the 3D-PSD housing material at five-time points (24, 48, 96, 144, and 192 h for $n = 3$ devices tested per timepoint). Additional details are given in S1.

2.5. 3D-PSD construction, calibration, and extraction procedures

HLB-type disks comprising divinylbenzene with hydrophilic moieties and Supor poly(ether sulfone) (PES) 0.2 mm membranes were sourced from Affinisep (Val de Reuil, France) and Pall Europe Ltd. (Portsmouth, UK), respectively. Both the HLB disks and PES membranes were cut to 9 mm disks (surface area = 0.5 cm^2) using a clean, dry wad punch and conditioned before deployment with 5 mL of MeOH and ultrapure water. Any manufacturing residues were removed from the PES membranes with two sequential 24-hour MeOH washes (Guibal et al., 2015). Each 3D-PSD contained five sorbent disks and was assembled for deployment by first placing the PES membranes inside the top section (Fig. 1(c)) of the device with the HLB disks stacked on top of the PES. The base component (Fig. 1 (b)) containing the corresponding 'turrets' was then aligned and clicked together to form a tight interference fit of the sorbent and the PES membrane leaving the top surface exposed to the environment, see Fig. S1 for details. The assembled devices were stored in ultrapure water until deployment for maximum of 48 h.

The R_s represents the volume of water cleared of a contaminant per unit of time (mL day^{-1}). It is calculated from the ratio of the slope of the regression line ($M_s t^{-1}$, mass on sampler per time) over the mean concentration in the matrix (C_w) for the period for which the slope is linear (Eq. 1) (Vrana et al., 2005; Castle et al., 2018).

$$R_s = \frac{M_s}{C_w.t} \tag{1}$$

Static renewal R_s calibration was performed (Charriau et al., 2016). A large glass beaker was filled with 5 L AFW and spiked with a mix of 136 analytes in MeOH to give a concentration of 50 ng L^{-1} of each compound. No additional organic solvent was required to maintain analyte solubility in AFW. Twelve 3D-PSD assemblies were used in all ($n = 60$ individual 9 mm sampling disks). For tank mounting, threaded 3D-printed "key" fittings were attached to zinc plated, threaded rods with bolts (M8 x 1 m,
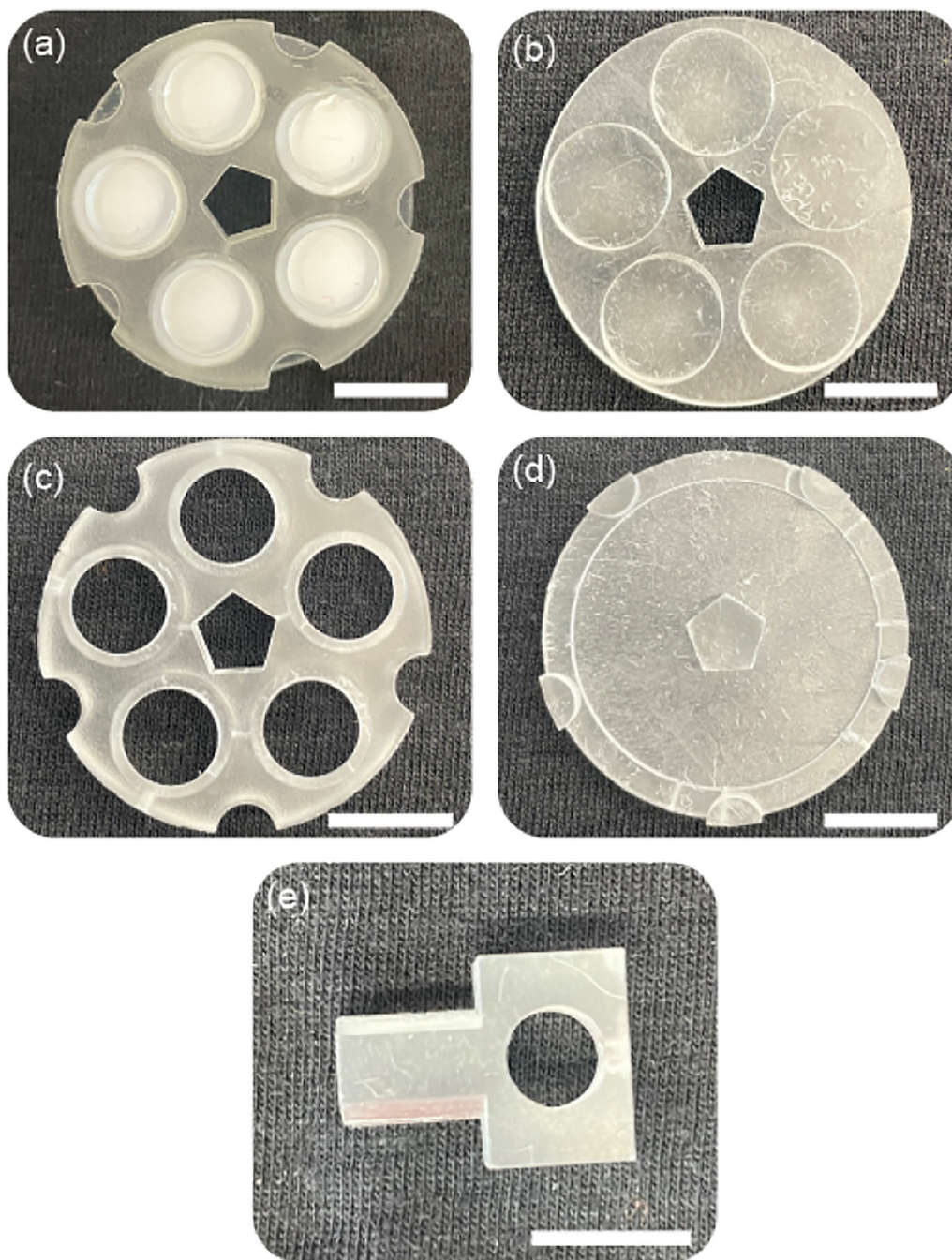
Fig. 1. Photographs of the assembled 3D-printed passive sampler (a) and the components manufactured in PlasCLEAR including (b) the base, (c) the top, (d) the transport cap and (e) the mounting key used for in-lab calibration studies. White bars represent 10 mm scale relative to each image.

Toolstation UK) that were then connected to 3D-PSDs at 6 cm intervals via their hexagonal central hole (Fig. 1 (e)). Fishing line was also used to further secure them, metal wire was not used as chemical sorption to the fishing line was considered negligible. Four rods were used in the same beaker, each with three 3D-PSDs. All rods were positioned 3 cm from the central rotation point of a central magnetic stirrer with 3D-PSDs facing inwards and therefore parallel with the flow (sampler face was ~2.5 cm from the centre of rotation, Fig. S2) (Ahkola et al., 2015). The stirrer was set to deliver a calculated flow velocity of 0.5 ± 0.1 m s^{-1} around all samplers according to Halász et al., which was similar to that observed in local rivers in the London area (Halász et al., 2007; NRFA, n.d.; Havery, 2016). The 3D-PSDs were deployed in the exposure beaker for the following time intervals: 8, 24, 48, 72, 96, 120, 144, 168, 192, 216, 240, and 264 h. At each time point, a single random 3D-PSD was removed. A 30 mL sample of water

was collected from the exposure tank at the same time as the 3D-PSD retrieval and an unused 3D-PSD was exposed to air and handling during manipulation. Extracts of this unused 3D-PSD were used as a negative control. Following collections at each interval, the spiked AFW was replaced. The sorbent disks and membranes were removed from the device and allowed to air dry overnight on MeOH-washed aluminium foil together with the negative control. Once dry, the HLB disks and PES membranes, as well as the corresponding water samples were stored at -20 °C until extraction.

Extraction was based on the method of Taylor et al., but was scaled down by HLB disk weight enabling a standard SPE vacuum manifold to be used (Taylor et al., 2020). Disks were placed in an empty fritted (polypropylene, 20 μm pore size) SPE cartridges (Agilent Technologies UK Ltd., Cheshire, UK) and configured to the manifold. With the

vacuum off and taps closed, 1 mL of MeOH was added to each cartridge and allowed to soak for 15 min, during which time no significant evaporation was noted. The taps were then opened and the MeOH was allowed to percolate under gravity into pointed glass tubes (15 mL, Merck Life Science UK Ltd., Dorset, UK). Following this, an additional 0.6 mL of MeOH was added to each cartridge under vacuum. Extracts were evaporated to dryness at 35 °C under N_2 before reconstitution in 200 µL of LC-MS mobile phase A. Details of extraction efficiency and recovery data are shown in S3 and Table S3. For quantification, calibrants were prepared by soaking fresh 3D-PSDs in AFW for 24 h, followed by direct spiking of the sorbent disks with analytical standards to form a nine-point calibration series (0.005 to 1 ng disk^{-1}). Each standard was analyzed in triplicate. The preparation of water samples for analysis is described in Richardson et al., (2021).

2.6. Procedures for field deployment in the River Wandle, London, UK

To prioritise 3D-PSD deployment locations, water samples were taken for analysis at four locations on the River Wandle in Greater London in April 2021. The River Wandle is a freshwater urban river that originates in Croydon, South London and flows through the boroughs of Sutton, Merton, and Wandsworth before joining the River Thames in Central London. Nineteen water samples were taken for analysis at various locations in Ravensbury Park, Poulter Park, Beddington Park, and Richmond Green. High resolution grab sampling (<200 m between points) was conducted at three of these sites and a single sample was taken at Ravensbury Park (see Table S4 and Table S5 for details, sites labelled A – S in Fig. 2). At each site, a 30 mL sample of river water was collected in pre-rinsed Nalgene® bottles (Sigma-Aldrich). External matrix-matched calibration
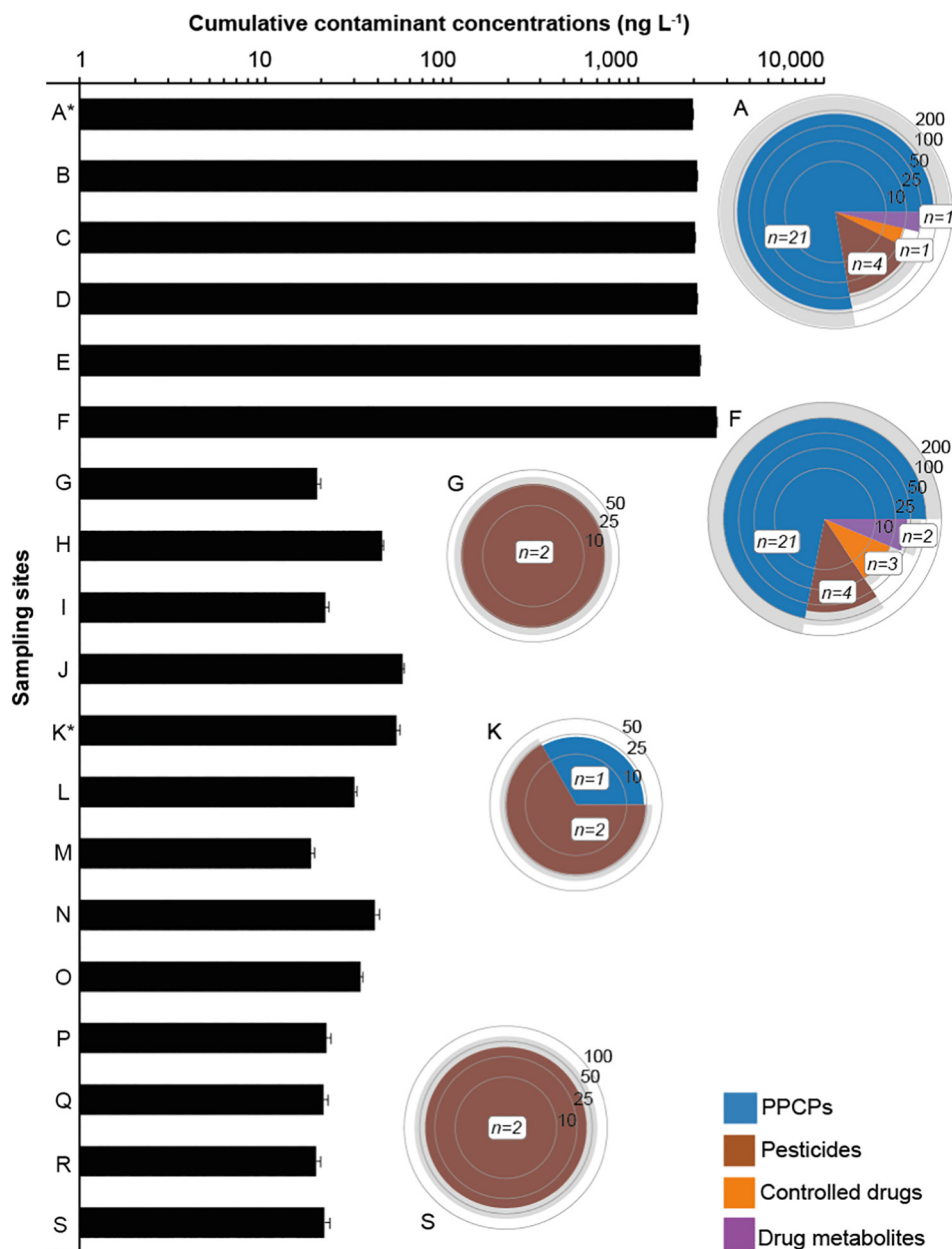
Fig. 2. Total CEC concentrations at all 19 River Wandle sampling sites in April 2021 measured using direct-injection LC-MS/MS of grab samples, positive error bars represent the standard error of the standard deviation across all CEC concentrations at that site. Sites are in descending order moving upstream from A to S towards the source. Sites A and K are marked with an * and represent the locations chosen for 3D-PSD deployment. Insert pie charts represent the mean concentrations (ng L^{-1}) of compound classes detected at selected sites (A, F, G, K, and S), standard deviation in grey. Concentric rings represent concentrations on a log scale. The number of compounds within each class is also indicated. Individual concentrations in both ng L^{-1} and pmol L^{-1} for all CECs detected at each site are given in Tables S4 & S5.

was used for quantification purposes and prepared using pooled river water samples created from combining equal volumes (700 μL) of water from all sites. A 14-point calibration curve (10 to 2000 ng L^{-1}) was created as per the method described in Richardson et al., (2021). In brief, 900 μL of river water was spiked with 100 μL of the analytical standard concentration required and SIL-IS (500 ng L^{-1}). Background subtraction in the matrix was done before any quantification was performed. That is, a blank, unspiked polled matrix was measured ($n = 3$, twice in the sequence) and the average peak area was removed from the measurements made in other calibration points. Standard addition calibration for each sample was not considered practical in this case given the number of samples required to be quantified. The calibrant samples was briefly vortexed before filtering into a deactivated HPLC vials (Agilent A-Line) through a 0.2 um polytetrafluoroethylene (PTFE) membrane using a BD Plastipak™ syringe (FisherScientific UK Ltd., Loughborough, UK).

Following the analysis of the river water, a site downstream of the WWTP effluent point (at Ravensbury Park, site A; 51.395227; −0.175981) and a background site upstream of the WWTP (at Beddington Park; site K; 51.372588; −0.147129) were selected for the deployment of the 3D-PSDs from the 4th to 11th June 2021. Selection of these sites was also based on safe access to the river and ability to anchor PSDs securely to the riverbed. Two 3D-PSDs were deployed at site A and five deployed at site K (i.e., to provide enough extract to prepare a matrix-matched calibration series). A separate field blank (an assembled 3D-PSD containing $n = 3$ HLB sorbent disks) was exposed to the air and handling of the samplers during deployment and retrieval. For deployment, the 3D-PSDs were fitted onto U-shaped galvanized garden pegs (15 × 0.29 cm, G&B, UK). The pegs were pushed into the riverbed with the sampler itself located above the riverbed surface. Upon retrieval, the 3D-PSDs were removed and rinsed with river water. The transport cap was fitted before wrapping the samplers in aluminium foil and storing them in a clean plastic container. 3D-PSDs were transported in a cool box to the laboratory, where they were disassembled, dried, stored, and extracted as per Section 2.5. For 3D-PSD quantification, matrix-matched calibrants were prepared by directly spiking spare sorbent disks from site K with analytical standards over the range of 0.005 to 10 ng disk^{-1}. Water samples were taken from each site (30 mL) at deployment and retrieval. All water samples were stored in a cool box during transport and stored at −20 °C at the laboratory until analysis. A flow-chart of the extraction and quantification process is shown in Fig. S3 including the types of data retrieved from analysis of water and passive sampler extracts.

3. Results and discussion

3.1. 3D-PSD device design and characterization

The final 3D-PSD design comprised two core parts; the top and base (Fig. 1(b) & (c)) and a third transport cap part (Fig. 1(d)) used during deployment and retrieval to protect the sorbent disks from contamination (see Fig. S4 for measurements). The interference fit increased the simplicity of the 3D-PSDs and a tight fit was still achievable for more than ten deployments across various projects. Threaded fittings were briefly explored but were deemed inferior due to inconsistencies in the build quality, friction wear, and difficulty removing sediment during cleaning, making sampler re-use impractical. The flat surface of the top reduced the water turbulence and the circular configuration ensured that the sorbent disks were exposed to similar local conditions in the water column (Ahkola et al., 2015). Print reproducibility between the devices was high (<2% RSD in weight and all dimensions, $n = 15$) and there was no significant difference in dimensions between individual builds or builds before and after the post-cure process.

SEM imaging of the cured resin revealed that the material was nonporous, with no evidence of delamination or microscopic void formation in the final 3D parts (Fig. S5). The 3D printed devices are non-porous since there was no visual evidence of macropores on the surfaces, and the absence of micropores and mesopores was confirmed by BET analysis

(Fig. S6). Therefore, leaching of water through the walls of the device to reach the sorbent was unlikely.

Mean loss due to analyte sorption to the 3D-PSD housing across eight days in AFW and for all compounds, was 28 ± 40% (median = 12%). Controls were used to account for analyte loss due to sorption to the nalgene bottles, volatility and degradation. Seventy-seven compounds showed no or low sorption (<15%) to the 3D-PSD over this time (Fig. S7 (a)). Compounds that displayed some degree of sorption to the 3D-PSD ($n = 59$) (Fig. S7 (b)) had a range of physico-chemical properties but was generally higher for CECs with logD >2. For these compounds, the majority of losses occurred within the first 48 h of exposure (53 ± 28%). Of all ten 3D-printed resins evaluated in previous work, PlasCLEAR was the most suitable in terms of compatibility with organo-aqueous solvents, but a potential solution would be to manufacture this same PSD design from, for example, PTFE using alternative manufacturing methods (Irlam et al., 2020). Furthermore, preliminary work suggests that it is possible to extract sorbed compounds off the PlasCLEAR resin (results not shown), but further work is needed. A detailed discussion is given in S4 and sorption profiles in Fig. S8.

3.2. 3D-PSD in-laboratory calibration

Previous work by our group in the Thames estuary during a summer campaign revealed an average concentration of 47 ± 49 ng L^{-1} for 33 CECs (Richardson et al., 2021). Therefore, a similarly low (50 ng L^{-1}) and environmentally relevant exposure concentration was chosen to show the benefits of the 3D-PSD approach coupled with a rapid and sensitive direct injection LC-MS/MS method for water samples at environmentally relevant concentrations. The actual CEC concentration was measured during the exposure and remained consistent at 36 ± 6 ng L^{-1} over daily renewal of freshly prepared spiked AFW matrix.

R_s values were reliably determined for 39 compounds in this initial development work (Table 1), though it is envisaged that substantially more could be determined if higher exposure concentrations were employed. Generally, the uptake onto the 3D-PSD was linear up to 11 days (Fig. 3 & S8 for individual compounds). Using this methodology, it was decided to limit the 3D-PSD deployment period to seven days to ensure that all compounds remained in the linear uptake range. R_s values ranged from 0.3 mL day^{-1} (propamocarb) to 12.3 mL day^{-1} (carbamazepine). There was no correlation between compound logD, logP, and R_s, in line with the observations of other studies (Petrie et al., 2016; Gunold et al., 2008; Moschet et al., 2015; Shaw et al., 2009). LogD and logP were calculated using the Percepta PhysChem Profiler software (ACD Laboratories, Ontario, Canada). The mean TWA limit of detection (LOD, defined as 3.3 times the standard deviation of the y-intercept divided by the slope according to ICH guidelines) and lower limit of quantification (LLOQ, defined as 3 times the LOD) across all compounds retained on the sampler was 0.5 ± 0.6 ng L^{-1} (Table 1) and 1.4 ± 1.9 ng L^{-1}, respectively based on a seven day exposure (ICH expert working group, 2005). The LOD/LLOQ values were extrapolated from a spiked ng disk^{-1} value, calculated as per above, to ng L^{-1} which is what would be experienced by the 3D-PSD in environmental waters using the calculated R_s over a period of seven days. Estimated LOD/LLOQ values for the spiked 3D-PSD all lay within the range of the calibration line and were verified in all cases. In terms of LOD, this represents a significant improvement in sensitivity (($p<0.05$) by 86% (4 ng L^{-1}, on average)) when compared to direct measurement of AFW.

3.3. Effects of reducing the surface area of a PSD

Uptake follows first-order kinetics and is described using a one-compartment model (Eq. (2)). The concentration on-sampler is determined by the partition coefficient between the sampler and the exposure matrix (K_{SM}), concentration in the matrix, the total mass transfer coefficient (h_0), time (t), and the sampling area and volume of a sampler, A_s and V_s,

respectively (Taylor et al., 2019; Salim and Górecki, 2019; Vrana et al., 2007; Vrana et al., 2006).

$$M_s = K_{SM} C_w \left(1 - \exp\left(-\left(\frac{h_0 A_s}{V_s K_{SM}}\right) t \right) \right) \tag{2}$$

During the initial linear, kinetic region, the analyte concentration on the sampler is insignificant, thus Eq. (2) is reduced to:

$$M_s = h_0 A_s C_w t \tag{3}$$

Table 1

Regression information and $R_s \pm$ standard deviation (SD) for the 3D-PSD and compared to literature-reported Chemcatcher® R_s. HLB R_s data are underlined for clarity.

Compound	AFW[¥] LOD (ng L⁻¹)	3D-PSD LOD pg disk⁻¹	LOD ng L⁻¹[†]	Linear range (d)	R²	$R_s \pm$ SD (mL d⁻¹) (normalized surface area)[‡]	Literature R_s (mL d⁻¹) In lab Freshwater	In lab Effluent	In situ Freshwater	In situ Effluent
Amphetamine	5	5	0.4	1–11	0.82	1.6 ± 0.1 (48)	–	–	–	28[c,vii]
Azoxystrobin	4	9	0.1	1–11	0.77	10.2 ± 0.8 (309)	580[a,viii],770[a,iii]	–	–	–
Benzatropine	4	36	2	1–11	0.80	3.2 ± 0.1 (96)	–	–	–	–
Benzoylecgonine	4	8	0.1	0.3–11	0.87	8.5 ± 0.7 (259)	–	–	30[a,vi]	–
Bisoprolol	4	2	0.1	0.3–11	0.81	3.7 ± 0.3 (114)	–	–	–	–
Buspirone	4	29	2	4–11	0.97	2.4 ± 0.4 (72)	–	–	–	–
Carazolol	3	1	<0.1	0.3–11	0.82	4.9 ± 0.5 (150)	–	–	–	–
Carbamazepine	4	6	0.1	0.3–11	0.85	12.3 ± 1.0 (375)	98[a,xi],340[a,x], 770[a,x],850[a,v], 1070[a,v]	–	100[a,vi]	45[c,vii]
Carbamazepine-10,11-epoxide	4	2	0.1	0.3–11	0.88	4.2 ± 0.4 (128)	–	–	100[a,vi]	–
Citalopram	5	33	3	3–11	0.99	1.6 ± 0.2 (48)	–	–	–	69[c,vii]
Dimethametryn	4	10	0.4	1–10	0.93	3.4 ± 0.9 (104)	–	–	–	–
Flutolanil	4	4	0.1	1–11	0.80	6.1 ± 0.6 (184)	–	–	–	–
Fuberidazole	4	8	0.1	1–11	0.75	8.3 ± 0.6 (254)	–	–	–	–
Isocarbamid	4	4	0.1	0.3–11	0.89	6.3 ± 0.5 (191)	–	–	–	–
Ketamine	4	6	0.3	1–11	0.71	2.7 ± 0.1 (81)	–	–	–	–
Ketotifen	4	15	2	3–11	0.84	1.3 ± 0.2 (39)	–	–	–	–
Lidocaine	4	1	0.2	0.3–6	0.96	0.8 ± 0.1 (23)	–	–	90[a,vi]	–
MDMA	4	8	0.3	1–11	0.69	3.3 ± 0.4 (100)	–	–	–	74[c,vii]
Memantine	4	5	0.1	0.3–11	0.87	6.0 ± 0.3 (181)	–	–	–	–
Mephosfolan	4	1	<0.1	0.3–11	0.86	6.7 ± 0.5 (203)	–	–	–	–
Methamphetamine	4	7	0.7	1–11	0.78	1.4 ± 0.1 (41)	–	–	–	25[c,vii]
Metoprolol	4	3	0.1	0.3–11	0.78	4.1 ± 0.4 (125)	–	–	–	50[c,vii]
Oxycodone	4	1	0.1	0.3–11	0.77	2.8 ± 0.3 (85)	–	–	–	–
Pirenzipine	4	10	2	1–11	0.84	1.0 ± 0.1 (30)	–	–	–	–
Propamocarb	4	3	1	0.3–7	0.71	0.3 ± 0.2 (10)	3[b,ii], 20[a,viii], 30[a,ii]	–	1.3[b,i]	–
Pymetrozine	4	7	0.3	0.3–11	0.89	3.5 ± 0.4 (107)	–	–	–	–
Pyracarbolid	4	20	0.5	1–11	0.78	5.4 ± 0.4 (165)	–	–	–	–
Ronidazole	4	4	0.3	0.3–11	0.90	2.1 ± 0.2 (62)	–	–	–	–
Salbutamol	4	13	0.4	0.3–11	0.81	4.8 ± 0.6 (147)	–	–	–	–
Sulfamethazine	4	22	0.5	0.3–11	0.86	6.1 ± 0.6 (184)	–	–	100[a,vi]	–
Sulfapyridine	4	20	0.5	0.3–11	0.87	6.0 ± 0.7 (183)	–	–	100[a,vi]	–
Tacrine	4	6	0.1	0.3–11	0.85	11.9 ± 1.1 (363)	–	–	–	–
Tamsulosin	4	5	0.1	1–11	0.76	8.1 ± 0.5 (245)	–	–	–	–
Temazepam	4	4	0.1	0.3–11	0.80	8.2 ± 0.6 (248)	–	–	–	326[c,vii]
Terbutryn	4	4	0.1	0.3–10	0.89	6.1 ± 1.0 (186)	20[b,ii], 20[a,ii], 65[a,v], 81[a,xi], 380[a,x],790[a,xi]	110[a,ix]	46[c,iv]	–
Tramadol	4	3	0.2	1–11	0.67	1.9 ± 0.3 (58)	–	–	–	47[c,vii]
Trimethoprim	4	4	0.1	0.3–11	0.85	6.3 ± 0.5 (192)	–	–	30[a,vi]	28[c,vii]
Venlafaxine	4	8	0.7	1–11	0.73	1.6 ± 0.3 (48)	–	–	10[a,vi]	65[c,vii]
Verapamil	4	11	0.4	3–11	0.63	3.7 ± 0.5 (113)	–	–	–	–

[†] LOD based on a seven-day deployment.

[‡] R_s normalized to Chemcatcher® surface area by multiplying by the fold difference between the PSDs (30.4).

[a] SDB-RPS.

[b] C18.

[c] HLB.

[¥] Artificial fresh water (AFW) prepared as per the OECD Test Guideline No.203 by diluting stock solutions of $CaCl_2$, $MgSO_4$, $NaHCO_3$, and KCl to 2.0 mM, 0.50 mM, 0.77 mM, and 0.07 mM.

[i] Ahrens et al., 2018.

[ii] Ahrens et al., 2015.

[iii] Fernández et al., 2014.

[iv] Grodtke et al., 2020.

[v] Kaserzon et al., 2014.

[vi] Moschet et al., 2015.

[vii] Petrie et al., 2016.

[viii] Schreiner et al., 2020.

[ix] Vermeirssen et al., 2009.

[x] Vermeirssen et al., 2013.
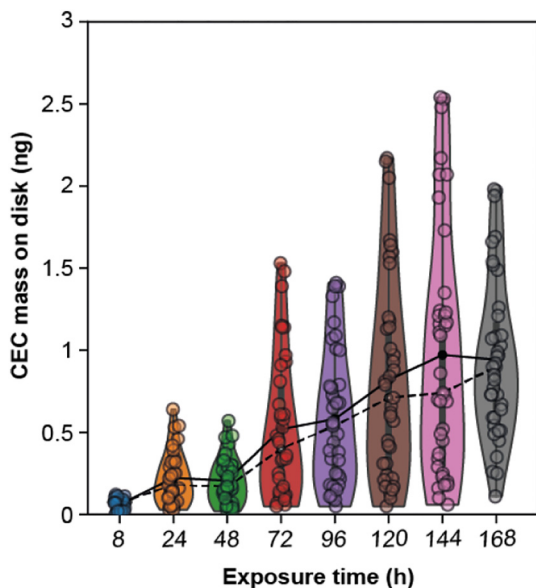
[xi] Vermeirssen et al., 2012.

Fig. 3. Violin plot of in-lab uptake for all compounds ($n = 39$) over seven days, mean and median values are represented by the solid and dashed lines, respectively. Individual compound uptake curves can be found in S9.

and, where h_0A_s describes the sampling rate (R_s), Eq. (1) (Salim and Górecki, 2019).

Therefore, reducing the size of the passive sampler will result in a lower R_s. It is difficult to compare R_s values between studies as it is well documented that R_s is affected by abiotic factors, such as temperature and water velocity (Vrana et al., 2005; Roll and Halden, 2016). Published work also uses a range of different receiving phases and formats other than HLB and this may have an effect on compound uptake, which can make directly comparing R_s values problematic (Becker et al., 2021). The 3D-PSD active sampling area was 0.50 cm^2, which was approximately 30-fold smaller than the Chemcatcher® (15.2 cm^2) (Gravell et al., 2020). Therefore, as expected, the R_s values calculated were lower by comparison (Table 1) (Grodtke et al., 2020; Petrie et al., 2016; Moschet et al., 2015; Ahrens et al., 2018; Ahrens et al., 2015; Kaserzon et al., 2014; Schreiner et al., 2020; Vermeirssen et al., 2013; Fernández et al., 2014; Vermeirssen et al., 2009; Vermeirssen et al., 2012). Differences in R_s between PSDs with different surface areas have reported previously (Gravell et al., 2020; Ahrens et al., 2015; Kaserzon et al., 2014; Gong et al., 2018; Challis et al., 2020; Buzier et al., 2019). However, not all devices have clearly defined surface areas. Gravell et al. reported that POCIS devices exhibited larger R_s than Chemcatcher® (Gravell et al., 2020). However, it was noted that differences were smaller than expected based on the ratio of sampling areas between the two devices, potentially due sorbent particle mobility (Gravell et al., 2020). Buzier et al. reported lower sensitivity of o-DGT devices when compared to POCIS devices under similar flow conditions due to differences in sampling areas (Buzier et al., 2019). When R_s for the 3D-PSD were normalized to the larger surface area of the Chemcatcher® it was clear these were broadly similar to a range of published R_s, even across a variety of sorbents (Table 1).

3.4. River water analysis and targeted 3D-PSD field deployment

Analysis of water samples from 19 sites along the River Wandle during April 2021 was used to locate a source of chemical contamination for subsequent 3D-PSD deployment. Targeted analysis of water samples using direct-injection LC-MS/MS identified 48 unique compounds, 32 of which were quantifiable (Table S4 & Table S5). Compounds were categorized into pharmaceuticals and personal care products (PPCPs), pesticides, controlled drugs, and drug metabolites. Of the compounds detected, six (atrazine, simazine, sulfamethoxazole, terbutryn, trimethoprim, and

venlafaxine) are/have been on the European WFD Watch/Priority substances lists (European Commission, 2015; European Commission, 2013). The discharge point from the Beddington wastewater treatment plant (WWTP) was identified at site F (51.387923, −0.165262) in Fig. 2. Upstream of this point, 19 unique compounds were detectable across 13 sites, with an average concentration of 23 ± 10 ng L^{-1} (median = 19 ng L^{-1}) or 145 ± 87 pmol L^{-1}. Downstream, 47 unique compounds were present at six locations, with an average concentration of 70 ± 78 ng L^{-1} (median = 35 ng L^{-1}), or 292 ± 312 pmol L^{-1}. Twenty-six PPCPs were quantifiable at all sites downstream of site F (Table S4 & Table S5) and eight (carbamazepine, diclofenac, propranolol, sulfamethoxazole, sulfapyridine, temazepam, tramadol, and trimethoprim) of these have been previously reported in the effluent from another major London treatment works (Munro et al., 2019). Controlled drugs including amphetamine, MDMA, and ketamine were also quantifiable in sites downstream of site F. The cocaine metabolite benzoylecgonine (BZE) was quantifiable at site F, but fell below the LLOQ further downstream and has been previously shown to be a suitable marker of wastewater overflows (Munro et al., 2019). The metabolite carbamazepine-10,11-epoxide (CBZ epoxide) was present at all downstream sites along with its parent, carbamazepine, at all except one site. Of all compounds detected, six (bezafibrate, carbamazepine, metoprolol, propranolol, temazepam, and trimethoprim) were relatively consistent with previous studies monitoring the surface waters of the River Wandle (Miller et al., 2015; Egli et al., 2021).

Following this, two sites were selected for the deployment of 3D-PSDs and using the reduced-scale workflow. The first impacted location (site A) was ~1.5 km downstream of the wastewater treatment plant (WWTP) discharge point. The second location (site K) was in Beddington Park ~3 km upstream of the WWTP and receives drainage from the London borough of Croydon (Schnell et al., 2015). All 3D-PSDs were retrieved from site A, but only three were retrieved from site K due to two devices missing (i.e., resulting in $n = 15$ disks in total). Targeted analysis of river water collected during deployment and retrieval identified 42 unique compounds across both sites. Of these, 32 were quantifiable above the LLOQ (Tables S6 & S7). Five contaminants identified (atrazine, sulfamethoxazole, terbutryn, trimethoprim, and venlafaxine) are/have been on the European WFD Watch/Priority substances lists (European Commission, 2015; European Commission, 2013).

Analysis of 3D-PSD extracts from the field are also shown in Tables S6 and S7. Across both sites, 80 compounds were detected (56 common to both sites). In field blanks, 27 compounds were detectable. Where the peak intensities of the compounds in the field blanks was greater than 10% of the peak intensities from the site samples, these compounds were excluded as contamination could not be ruled out. Three compounds (antipyrine, cocaine and warfarin) were excluded because of this. A total of 38 (site A) and 32 (site K) compounds were detected in 3D-PSD extracts that were not detectable in the water samples. Three compounds (cyromazine, disulfoton sulfone and metoprolol) were detected in water that were not detected in the passive sampler extracts. The LogD of these compounds range from −0.25 (metoprolol) to 2.11 (disulfoton sulfone), therefore are unlikely to be fully eluted from the 3D-PSD using methanol. However, overall, the use of the 3D-PSD had clear advantages over grab sampling including the total number of compounds detected at higher sensitivity.

At site A, there were R_s values and quantifiable amounts in sampler extracts, to calculate TWA concentrations for 10 CECs. These together with CECs in the river water quantified at the start and end of the deployment period are shown in Table 2. It is not possible to accurately evaluate TWA concentrations obtained from passive sampler deployments with infrequent spot samples. However, except for lidocaine and venlafaxine, concentrations found between the two monitoring methods were generally similar. Eight compounds (bisoprolol, carbamazepine-10,11-epoxide, memantine, pirenzepine, salbutamol, sulfapyridine, temazepam, and trimethoprim) were in excellent agreement within an average of 23 ± 17 ng L^{-1}. Higher concentrations of lidocaine and venlafaxine (510 ± 99 ng L^{-1} and 725 ± 30 ng L^{-1}, respectively) were found in 3D-PSD extracts compared to grab water samples. Both are widely prescribed in the UK and both have

Table 2

Mean concentration of contaminants detected at site A in extracts from the 3D-PSD and in water samples collected at the deployment and retrieval of the samplers. Data are reported along with the standard deviation in parenthesis.

Compound	[CEC] on 3D-PSD[a] (ng disk^{-1})	[CEC] in river water (ng L^{-1})		R_s (mL d^{-1})	TWA of [CEC] in river water (ng L^{-1})[c]
		04 Jun 2021[b]	11 Jun 2021[a]		
Bisoprolol	1.4 (0.2)	31 (3)	35 (2)	3.7 ± 0.3	54 (9)
Carbamazepine-10,11-epoxide	3.4 (0.3)	57 (5)	75 (6)	4.2 ± 0.4	117 (9)
Lidocaine	2.7 (0.5)	93 (1)	107 (10)	0.8 ± 0.1	510 (99)
Memantine	1.1 (0.2)	22 (1)	24 (3)	6.0 ± 0.3	26 (5)
Pirenzepine	0.31 (0.1)	12 (3)	12 (3)	1.0 ± 0.1	45 (7)
Salbutamol	0.28 (0.1)	13 (1)	13 (1)	4.8 ± 0.6	8 (1)
Sulfapyridine	8.9 (0.7)	122 (4)	193 (17)	6.0 ± 0.7	210 (17)
Temazepam	1.1 (0.1)	26 (3)	27 (4)	8.2 ± 0.6	20 (2)
Trimethoprim	5.8 (1)	146 (10)	164 (18)	6.3 ± 0.5	131 (23)
Venlafaxine	8.1 (0.3)	348 (4)	221 (12)	1.6 ± 0.3	725 (30)

[a] $n = 6$.
[b] $n = 3$.
[c] TWA standard deviation was determined from $n = 6$ 3D-PSD replicates using the mean R_s value.

moderate to poor removal rates (e.g. lidocaine, 14–35% and venlafaxine, 37–56%) by activated sludge treatment at WWTPs (English Prescribing Dataset (EPD), 2020; Rúa-Gómez et al., 2012).

In particular, the grab samples were only taken at deployment and retrieval and in relatively dry weather. Rainfall in this area over the deployment period was 10.8 mm (UK Centre for Ecology and Hydrology, 2021). Therefore, any potential storm or sewage overflow events carrying additional loadings on CECs during the deployment period would not have been captured in these samples (Munro et al., 2019). Furthermore, differences between the two methods may also be due to the R_s value, which can be affected by water turbulence, temperature, and fouling of the PES membrane, all of which are not replicated in laboratory calibrations (Taylor et al., 2020; Vrana et al., 2006). For example, Vrana and co-workers demonstrated that uptake rates for 18 compounds at three different temperatures (6, 11, and 18 °C) using the Chemcatcher® device increased with temperature (Vrana et al., 2006).

Based on grab sample measurements and 3D-PSD determinations, six substances yielded risk quotients >0.1 (Table S8, calculated as per Egli et al.) (Egli et al., 2021). Moderate to high risks were calculated for trimethoprim and venlafaxine in particular (Table S8), and both have been shown to pose risks in other rivers previously including in the UK and have been shortlisted considered for inclusion in the 3rd EU Watch List (Egli et al., 2021; Evans et al., 2017; Castillo-Zacarías et al., 2021; Gomez Cortes et al., 2020).

3.5. Suspect screening of 3D-PSD extracts

Following targeted LC-MS/MS analysis, the same extracts from sites A (downstream of Beddington WWTP) and K (upstream of Beddington WWTP) were subjected to suspect screening analysis by LC-QTOF-MS. As a qualitative tool, the new 3D-PSD workflow showed a distinct capability to detect a much larger range of chemically diverse compounds on top of those detected using targeted LC-MS/MS. In total, and across both sites, 113 additional compounds were identified based on LC and HRMS library data matching (Table S9). This included 20 pesticides, seven pesticide transformation products, 69 pharmaceuticals, 12 pharmaceutical metabolites, three controlled drugs and two controlled drug metabolites. A difference between extracts up and downstream of the WWTP was observed (34 compounds detected versus 98, respectively). Taking pharmaceuticals as an example, and in addition to those identified by the targeted method, this number of compounds suggests that CEC contamination could far-exceed those reported even in recent monitoring programmes in rivers, including in the London area (Richardson et al., 2021; Wilkinson et al., 2022). Therefore, such 3D-PSD tools could offer a more realistic assessment of environmental CEC occurrence at scale and minimise the need for shipping liquid samples internationally. Of the compounds detected, it was particularly useful to note high frequency occurrence of four additional

compounds currently being considered for inclusion onto the 3rd EU Watch List for rivers including fluconazole, desmethylvenlafaxine, imazalil and propiconazole (Cortes et al., 2020). Occurrence was generally more frequent and at higher intensity for three of these compounds downstream of the WWTP at site A. As an example, LC-QTOF-MS data for the antifungal fluconazole is shown in Fig. 4(a), where matches to library reference data were clearly obtained. Also worthy of note was the occurrence of a veterinary parasiticide, fipronil (Fig. 4(b)). It was detected in all extracts, but higher signal intensity was recorded at site A (Table S9). Intermittent detection of its transformation product fipronil sulfone was also recorded in extracts also at both sites. This compound is also to be considered in subsequent iterations of the EU Watch List given its toxicity at low concentrations (Wang et al., 2022; Monteiro et al., 2019). In England, semi-quantitative data exists for fipronil at concentrations of 10 ± 20 ng L^{-1} (for measurements between 2013 and 2021), indicating the high degree of sensitivity and replication capability offered by this small device (Water quality monitoring data GCMS LCMS Semiquantitative, 2021). Other frequently occurring compounds worthy of note include the transformation products/metabolites of parent compounds already detected in the targeted LC-MS/MS analysis including desethylatrazine, desmethylcitalopram, O-desmethyltramadol, codeine and cotinine. Upstream of the WWTP, a total of 15 unique compounds were shortlisted during suspect screening. Of these, positive detection in all three 3D-PSD disks tested was obtained for seven compounds (carbendazim, O-desmethylvenlafaxine, DMST, psilocyn, pyrimethanil, tolmetin and yangonin). Therefore, overall, the new reduced scale passive sampling workflow was considered an excellent means to enable convenient shortlisting of large numbers of CECs and related compounds with more replicates per device to add confidence.

3.6. Implications for the use of a 3D-PSD in CEC occurrence monitoring

Despite lower sensitivity inherent to the smaller disk sampling areas, there are several advantages to this methodology overall. Firstly, these represent a significant cost reduction for PSDs with materials for a single device costing under £10 (see Table S10 for materials costs) when compared to a commercial Chemcatcher® device. Three 3D-PSD devices containing five disks each can be assembled from a single 47 mm sorbent disk, making replication more convenient and potentially more accessible for larger-scale programs. Its size made large batches easier to transport to site and also to conceal during deployment, which mimimised loss from public interference (the housing material itself is colourless and remains so throughout deployment and can be restored to its original condition with solvent washing after deployment). Utilizing 3D-printed parts allows devices to be printed on-demand, thus saving lead time in production and delivery, as *.STL files can be easily shared between collaborators. The device can also be easily modified to include the functionality and

Fig. 4. Example precursor extracted ion chromatograms and mirrored DIA-MS/MS spectra for 3D-PSD extracts and their reference MS/MS spectra using LC-QTOF-MS for (a) fluconcazole and (b) fipronil.

performance of other available PSDs if needed, such as POCIS and DGT devices, and/or multiple different sorbent chemistries.

Finally, the 3D-PSD is in line with the principles of green analytical chemistry as outlined by Gałuszka et al., particularly points five (automated and miniaturized methods should be selected), seven (generation of a large volume of analytical waste should be avoided), and eight (multi-analyte or multi-parameter methods are preferred versus methods using one analyte at a time) (Gałuszka et al., 2013). The miniaturized nature of the 3D-PSD significantly reduces the amount of solvent waste generated. By comparison to Chemcatcher®, the 3D-PSD used only 1.6 mL methanol for extraction of a single sorbent disk, representing a 25-fold reduction (Richardson et al., 2021; Petrie et al., 2016). The device can also be multiplexed with different sorbent chemistries within the same location in the water column, allowing simultaneous capture of anions, cations, nutrients, metals, for example, and will be the focus of future work. In addition to the device itself, the rapid LC-MS/MS analytical method also carries significant benefits including enhanced sensitivity potentially to overcome issues with a smaller PSD sampling area. A total of 260 injections could be performed in any 24-hour period with a total solvent consumption of 2.8 mL per injection. Furthermore, aside from sample filtration, no pre-concentration steps were required and it, therefore, minimized or eliminated the need for sorbent-packed SPE cartridges for water analysis, large tailored exposure/extraction manifolds, and associated plastic/glassware for sample preparation using the 3D-PSD.

4. Conclusion

The miniaturization of a Chemcatcher®-type passive sampling and analytical workflow was successfully demonstrated for CEC monitoring and resulted in significant efficiency and practicality gains over existing approaches. A new prototype 3D-printed PSD held five sorbent disks and in-laboratory sampling rates (R_s) could be generated for 39 compounds. Sampling rates were smaller as a result of miniaturization, but a direct injection LC-MS/MS method enabled analysis of 164 CECs in water at the low ng L^{-1} concentration level to enable these to be calculated. Importantly, such high sensitivity using only 10 μL injection volumes supported a reduction in the size of associated PSD calibration equipment, solvent and reagents required. A 5 L beaker was sufficient to calibrate 12 PSDs containing 60 individual 9 mm diameter disks simultaneously. In terms of solvents and reagents, a 25-fold reduction in methanol for extraction of PSD disks was also achieved, along with lower amounts of reference materials for calibration. Identification of elevated wastewater-related CEC concentrations using targeted direct-injection LC-MS/MS along the river enabled identification of suitable sites for deployment of PSDs where 81 CECs, metabolites and transformation products were then detected over a weeklong deployment. Using suspect screening at two selected sites, a total of 113 additional unique compounds were detected in the same PSD extracts. Good agreement between PSD-estimated concentrations and measurements in water were obtained for 10 CECs for which R_s data were available. There were some limitations to this work, including (a) more R_s data are needed to widen its quantitative applicability, which could be achieved perhaps

with calibration at a higher exposure concentration (b) sorption to the passive sampler housing was not insignificant for less polar compounds and therefore, alternative materials should be sought to improve performance, perhaps using alternative materials beyond the current capabilities of widely available 3D-printing technology like this and; (c) miniaturizing the sampling area requires a higher sensitivity LC-MS/MS method and seemed to reduce deployable time of the sampler. However, overall, this improved workflow still represents a significantly more cost-effective and practical solution for time integrated CEC monitoring and helps to increase accessibility for analytical laboratories to passive sampling potentially at scale.

CRediT authorship contribution statement

Alexandra K. Richardson: Conceptualisation, Methodology, Validation, Formal analysis, Investigation, Data curation, Writing – original draft, Writing – review & editing. **Rachel C. Irlam:** Data curation, Investigation, Writing – original draft, Writing – review & editing. **Helena Rapp Wright:** Data curation, Writing – review. **Graham A. Mills:** Resources, Writing – review & editing. **Gary R. Fones:** Resources, Writing – review & editing. **Stephen Stürzenbaum:** Writing – review & editing, Supervision. **David A. Cowan:** Writing – review & editing, Supervision. **David J. Neep:** Resources, Investigation, Writing – review & editing, Supervision. **Leon P. Barron:** Conceptualisation, Resources, Writing – original draft, Writing – review & editing, Supervision, Project administration, Funding acquisition.

Declaration of competing interest

The authors declare that they have no known competing financial interests or personal relationships that could have appeared to influence the work reported in this paper.

Acknowledgments

Appendix A. Supplementary data

Supplementary data to this article can be found online at https://doi.org/10.1016/j.scitotenv.2022.156260.

References

Ahkola, H., Juntunen, J., Laitinen, M., Krogerus, K., Huttula, T., Herve, S., Witick, A., 2015. Effect of the orientation and fluid flow on the accumulation of organotin compounds to chemcatcher passive samplers. Environ. Sci. Process. Impacts 17 (4), 813–824. https://doi.org/10.1039/c4em00585f.

Ahrens, L., Daneshvar, A., Lau, A.E., Kreuger, J., 2015. Characterization of five passive sampling devices for monitoring of pesticides in water. J. Chromatogr. A 1405, 1–11. https://doi.org/10.1016/j.chroma.2015.05.044.

Ahrens, L., Daneshvar, A., Lau, A.E., Kreuger, J., 2018. Concentrations, fluxes and field calibration of passive water samplers for pesticides and Hazard-based risk assessment. Sci. Total Environ. 637–638, 835–843. https://doi.org/10.1016/j.scitotenv.2018.05.039.

Almeida, M.I.G.S., Silva, A.M.L., Coleman, R.A., Pettigrove, V.J., Cattrall, R.W., Kolev, S.D., 2016. Development of a passive sampler based on a polymer inclusion membrane for Total ammonia monitoring in freshwaters. Anal. Bioanal. Chem. 408 (12), 3213–3222. https://doi.org/10.1007/s00216-016-9394-2.

Alvarez, D.A., Petty, J.D., Huckins, J.N., Jones-Lepp, T.L., Getting, D.T., Goddard, J.P., Manahan, S.E., 2004. Development of a passive, in situ, integrative sampler for hydrophilic organic contaminants in aquatic environments. Environ. Toxicol. Chem. 23 (7), 1640. https://doi.org/10.1897/03-603.

Anderson, K.B., Lockwood, S.Y., Martin, R.S., Spence, D.M., 2013. A 3D printed fluidic device that enables integrated features. Anal. Chem. 85 (12), 5622–5626. https://doi.org/10.1021/ac4009594.

aus der Beek, T., Weber, F.A., Bergmann, A., Hickmann, S., Ebert, I., Hein, A., Küster, A., 2016. Pharmaceuticals in the environment-global occurrences and perspectives. Environ. Toxicol. Chem. 35 (4), 823–835. https://doi.org/10.1002/etc.3339.

Becker, B., Kochleus, C., Spira, D., Möhlenkamp, C., Bachtin, J., Meinecke, S., Vermeirssen, E.L.M.M., 2021. Passive Sampler phases for pesticides: evaluation of AttractSPETM SDB-RPS and HLB versus EmporeTM SDB-RPS. Environ. Sci. Pollut. Res. 28 (9), 11697. https://doi.org/10.1007/s11356-020-12109-9.

Boix, C., Ibáñez, M., Sancho, J.V., Rambla, J., Aranda, J.L., Ballester, S., Hernández, F., 2015. Fast determination of 40 drugs in water using large volume direct injection liquid chromatography-tandem mass spectrometry. Talanta 131, 719–727. https://doi.org/10.1016/j.talanta.2014.08.005.

Brack, W., Dulio, V., Ågerstrand, M., Allan, I., Altenburger, R., Brinkmann, M., Bunke, D., Burgess, R.M., Cousins, I., Escher, B.I., Hernández, F.J., Hewitt, L.M., Hilscherová, K., Hollender, J., Hollert, H., Kase, R., Klauer, B., Lindim, C., Herráez, D.L., Miège, C., Munthe, J., O'Toole, S., Posthuma, L., Rüdel, H., Schäfer, R.B., Sengl, M., Smedes, F., van der Meent, D., van den Brink, P.J., van Gils, J., van Wezel, A.P., Vethaak, A.D., Vermeirssen, E., von der Ohe, P.C., Vrana, B., 2017. Towards the review of the European union water framework management of chemical contamination in European surface water resources. Sci. Total Environ., 720–737 https://doi.org/10.1016/j.scitotenv.2016.10.104 Elsevier B.V. January 15.

Buzier, R., Guibal, R., Lissalde, S., Guibaud, G., 2019. Limitation of flow effect on passive sampling accuracy using POCIS with the PRC approach or O-DGT: a pilot-scale evaluation for pharmaceutical compounds. Chemosphere 222, 628–636. https://doi.org/10.1016/j.chemosphere.2019.01.181.

Caban, M., Lis, H., Stepnowski, P., 2021. Critical Reviews in Analytical Chemistry Limitations of Integrative Passive Samplers as a Tool for the Quantification of Pharmaceuticals in the Environment-A Critical Review with the Latest Innovations Limitations of Integrative Passive Samplers as a Tool. https://doi.org/10.1080/10408347.2021.1881755.

Castillo-Zacarías, C., Barocio, M.E., Hidalgo-Vázquez, E., Sosa-Hernández, J.E., Parra-Arroyo, L., López-Pacheco, I.Y., Barceló, D., Iqbal, H.N.M., Parra-Saldívar, R., 2021. Antidepressant drugs as emerging contaminants: occurrence in urban and non-urban waters and analytical methods for their detection. Sci. Total Environ. 757, 143722. https://doi.org/10.1016/J.SCITOTENV.2020.143722.

Castle, G.D., Mills, G.A., Bakir, A., Gravell, A., Schumacher, M., Townsend, I., Jones, L., Greenwood, R., Knott, S., Fones, G.R., 2018. Calibration and field evaluation of the Chemcatcher® passive sampler for monitoring metaldehyde in surface water. Talanta 179, 57–63. https://doi.org/10.1016/j.talanta.2017.10.053.

Challis, J.K., Almirall, X.O., Helm, P.A., Wong, C.S., 2020. Performance of the organic-diffusive gradients in thin-films passive sampler for measurement of target and suspect wastewater contaminants. Environ. Pollut. 261, 114092. https://doi.org/10.1016/j.envpol.2020.114092.

Chan, H.N., Chen, Y., Shu, Y., Chen, Y., Tian, Q., Wu, H., 2015. Direct, one-step molding of 3D-printed structures for convenient fabrication of truly 3D PDMS microfluidic chips. Microfluid. Nanofluidics 19 (1), 9–18. https://doi.org/10.1007/s10404-014-1542-4.

Charriau, A., Lissalde, S., Poulier, G., Mazzella, N., Buzier, R., Guibaud, G., 2016. Overview of the Chemcatcher® for the passive sampling of various pollutants in aquatic environments part a: principles, calibration, preparation and analysis of the sampler. Talanta, 556–571 https://doi.org/10.1016/j.talanta.2015.06.064 Elsevier February 1.

Chen, C., Wang, Y., Lockwood, S.Y., Spence, D.M., 2014. 3D-printed fluidic devices enable quantitative evaluation of blood components in modified storage solutions for use in transfusion medicine. Analyst 139 (13), 3219–3226. https://doi.org/10.1039/c3an02357e.

Cortes, L.G., Marinov, D., Sanseverino, I., Cuenca, A.N., Niegowska, M., Rodriguez, E.P., Lettieri, T., 2020. Selection of Substances for the 3rd Watch List under the Water Framework Directive.

EC, 2008. Directive 2008/56/EC of the European Parliament and of the Council of 17 June 2008 establishing a framework for community action in the field of marine environmental policy (marine strategy framework directive). Off. J. Eur. Union 026, 136–157.

Egli, M., Hartmann, A., Wright, H.R., Ng, K.T., Piel, F.B., Barron, L.P., 2021. Quantitative determination and environmental risk assessment of 102 chemicals of emerging concern in wastewater-impacted rivers using rapid direct-injection liquid chromatography—tandem mass spectrometry. Molecules 26 (18), 5431. https://doi.org/10.3390/MOLECULES26185431 2021, Vol. 26, Page 5431.

English Prescribing Dataset (EPD), 2020. NHS Bus. Serv. Auth. Data Wareh.

European Commission, 2013. Directive 2013/39/EU of the European parliament and of the council of 12 august 2013 amending directives 2000/60/EC and 2008/105/EC as regards priority substances in the field of water policy. Off. J. Eur. Union 226, 1–17.

European Commission, 2015. COMMISSION IMPLEMENTING DECISION (EU) 2020/1161 of 4 august 2020 establishing a watch list of substances for union-wide monitoring in the field of water policy pursuant to Directive 2008/105/EC of the European Parliament and of the Council. Off. J. Eur. Union 257 (40–42), 32–35.

European Commission, 2018. European Commission implementation decision 2018/840 establishing a watch list of substances for union-wide monitoring in the field of water policy pursuant to Directive 2008/105/EC of the European Parliament and of the Council and repealing commission im. Off. J. Eur. Union 61, 9–12.

Evans, S., Bagnall, J., Kasprzyk-Hordern, B., 2017. Enantiomeric profiling of a chemically diverse mixture of chiral pharmaceuticals in urban water. Environ. Pollut. 230, 368–377. https://doi.org/10.1016/J.ENVPOL.2017.06.070.

Fernández, D., Vermeirssen, E.L.M., Bandow, N., Muñoz, K., Schäfer, R.B., 2014. Calibration and field application of passive sampling for episodic exposure to polar organic pesticides in streams. Environ. Pollut. 194, 196–202. https://doi.org/10.1016/j.envpol.2014.08.001.

Gałuszka, A., Migaszewski, Z., Namieśnik, J., 2013. The 12 principles of green analytical chemistry and the SIGNIFICANCE mnemonic of green analytical practices. TrAC Trends Anal. Chem., 78–84 https://doi.org/10.1016/j.trac.2013.04.010 Elsevier B.V. October 1.

Gomez Cortes, L., Marinov, D., Sanseverino, I., Navarro Cuenca, A., Niegowska, M., Porcel Rodriguez, E., Lettieri, T., 2020. Selection of Substances for the 3rd Watch List under the Water Framework Directive; Luxembourg. https://doi.org/10.2760/194067.

Gong, X., Li, K., Wu, C., Wang, L., Sun, H., 2018. Passive sampling for monitoring polar organic pollutants in water by three typical samplers. Trends Environ. Anal. Chem., 23–33 https://doi.org/10.1016/j.teac.2018.01.002 Elsevier January 1.

Gravell, A., Fones, G.R., Greenwood, R., Mills, G.A., 2020. Detection of Pharmaceuticals in Wastewater Effluents—a Comparison of the performance of Chemcatcher® and polar organic compound integrative sampler. Environ. Sci. Pollut. Res. 27 (22), 27995–28005. https://doi.org/10.1007/s11356-020-09077-5.

Grodtke, M., Paschke, A., Harzdorf, J., Krauss, M., Schüürmann, G., 2020. Calibration and field application of the Atlantic HLB disk containing Chemcatcher® passive sampler – quantitative monitoring of herbicides, other pesticides and transformation products in german streams. J. Hazard. Mater. 124538. https://doi.org/10.1016/j.jhazmat.2020.124538.

Gross, B., Lockwood, S.Y., Spence, D.M., 2017. Recent advances in analytical chemistry by 3D printing. Anal. Chem., 57–70 https://doi.org/10.1021/acs.analchem.6b04344 American Chemical Society January 3.

Guibal, R., Lissalde, S., Charriau, A., Guibaud, G., 2015. Improvement of POCIS ability to quantify pesticides in natural water by reducing polyethylene glycol matrix effects from polyethersulfone membranes. Talanta 144, 1316–1323. https://doi.org/10.1016/j.talanta.2015.08.008.

Gunold, R., Schäfer, R.B., Paschke, A., Schüürmann, G., Liess, M., 2008. Calibration of the Chemcatcher® passive sampler for monitoring selected polar and semi-polar pesticides in surface water. Environ. Pollut. 155 (1), 52–60. https://doi.org/10.1016/j.envpol.2007.10.037.

Halász, G., Gyüre, B., Jánosi, I.M., Szabó, K.G., Tél, T., 2007. Vortex flow generated by a magnetic stirrer. Am. J. Phys. 75 (12), 1092–1098. https://doi.org/10.1119/1.2772287.

Havery, R., 2016. Thames Estuary Tidal Power Report.

Hermes, N., Jewell, K.S., Wick, A., Ternes, T.A., 2018. Quantification of more than 150 micropollutants including transformation products in aqueous samples by liquid chromatography-tandem mass spectrometry using scheduled multiple reaction monitoring. J. Chromatogr. A 1531, 64–73. https://doi.org/10.1016/j.chroma.2017.11.020.

ICH expert working group, 2005. Validation of Analytical Procedures: Text and Methodology Q2(R1). Int. Counc. Harmon. Tech. Requir. Pharm. Hum. Use (ICH).

Irlam, R.C., Hughes, C., Parkin, M.C., Beardah, M.S., O'Donnell, M., Brabazon, D., Barron, L.P., 2020. Trace multi-class organic explosives analysis in complex matrices enabled using LEGO®-inspired clickable 3D-printed solid phase extraction block arrays. J. Chromatogr. A 1629, 461506. https://doi.org/10.1016/j.chroma.2020.461506.

Kalsoom, U., Nesterenko, P.N., Paull, B., 2018. Current and future impact of 3D printing on the separation sciences. TrAC Trends Anal. Chem., 492–502 https://doi.org/10.1016/j.trac.2018.06.006 American Chemical Society January 3.

Kalsoom, U., Hasan, C.K., Tedone, L., Desire, C., Li, F., Breadmore, M.C., Nesterenko, P.N., Paull, B., 2018. Low-cost passive sampling device with integrated porous membrane produced using multimaterial 3D printing. Anal. Chem. 90 (20), 12081–12089. https://doi.org/10.1021/acs.analchem.8b02893.

Kaserzon, S.L., Hawker, D.W., Kennedy, K., Bartkow, M., Carter, S., Booij, K., Mueller, J.F., 2014. Characterisation and comparison of the uptake of ionizable and polar pesticides, pharmaceuticals and personal care products by POCIS and chemcatchers. Environ Sci Process Impacts 16 (11), 2517–2526. https://doi.org/10.1039/c4em00392f.

Miller, T.H., McEneff, G.L., Brown, R.J., Owen, S.F., Bury, N.R., Barron, L.P., 2015. Pharmaceuticals in the Freshwater Invertebrate, gammarus pulex, determined using pulverised liquid extraction, solid phase extraction and liquid chromatography-tandem mass spectrometry. Sci. Total Environ. 511, 153–160. https://doi.org/10.1016/j.scitotenv.2014.12.034.

Monteiro, H.R., Pestana, J.L.T., Novais, S.C., Leston, S., Ramos, F., Soares, A.M.V.M., Devreese, B., Lemos, M.F.L., 2019. Assessment of fipronil toxicity to the freshwater midge chironomus riparius: molecular, biochemical, and organismal responses. Aquat. Toxicol. 216, 105292. https://doi.org/10.1016/J.AQUATOX.2019.105292.

Moschet, C., Vermeirssen, E.L.M., Singer, H., Stamm, C., Hollender, J., 2015. Evaluation of in-situ calibration of chemcatcher passive samplers for 322 micropollutants in agricultural and urban affected Rivers. Water Res. 71, 306–317. https://doi.org/10.1016/j.watres.2014.12.043.

Munro, K., Martins, C.P.B., Loewenthal, M., Comber, S., Cowan, D.A., Pereira, L., Barron, L.P., 2019. Evaluation of combined sewer overflow impacts on short-term pharmaceutical and illicit drug occurrence in a heavily urbanised Tidal River catchment (London, UK). Sci. Total Environ. 657, 1099–1111. https://doi.org/10.1016/j.scitotenv.2018.12.108.

Namieśnik, J., Zabiegała, B., Kot-Wasik, A., Partyka, M., Wasik, A., 2005. Passive sampling and/or extraction techniques in environmental analysis: a review. Anal. Bioanal. Chem. 381 (2), 279–301. https://doi.org/10.1007/s00216-004-2830-8.

Ng, K.T., Rapp-Wright, H., Egli, M., Hartmann, A., Steele, J.C., Sosa-Hernández, J.E., Melchor-Martínez, E.M., Jacobs, M., White, B., Regan, F., Parra-Saldivar, R., Couchman, L., Halden, R.U., Barron, L.P., 2020. High-throughput multi-residue quantification of contaminants of emerging concern in wastewaters enabled using direct injection liquid chromatography-tandem mass spectrometry. J. Hazard. Mater. 398, 122933. https://doi.org/10.1016/j.jhazmat.2020.122933.

Nitti, F., Almeida, M.I.G.S., Morrison, R., Cattrall, R.W., Pettigrove, V.J., Coleman, R.A., Kolev, S.D., 2018. Development of a portable 3D-printed flow-through passive sampling device

free of flow pattern effects. Microchem. J. 143, 359–366. https://doi.org/10.1016/j.microc.2018.08.029.

Noguera-Oviedo, K., Aga, D.S., 2016. Lessons learned from more than two decades of research on emerging contaminants in the environment. J. Hazard. Mater. 316, 242–251. https://doi.org/10.1016/j.jhazmat.2016.04.058.

NRFA. National river flow archive https://nrfa.ceh.ac.uk/ (accessed Jun 16, 2021).

OECD, n.d. OECD Guidelines for Testing of Chemicals No. 203. Fish, Acute Toxicity Test; Paris.

Patel, M., Kumar, R., Kishor, K., Mlsna, T., Pittman, C.U., Mohan, D., 2019. Pharmaceuticals of Emerging Concern in Aquatic systems: chemistry, occurrence, effects, and removal methods. Chem. Rev. 119 (6), 3510–3673. https://doi.org/10.1021/acs.chemrev.8b00299.

Petrie, B., Gravell, A., Mills, G.A., Youdan, J., Barden, R., Kasprzyk-Hordern, B., 2016. In situ calibration of a new chemcatcher configuration for the determination of polar organic micropollutants in wastewater effluent. Environ. Sci. Technol. 50 (17), 9469–9478. https://doi.org/10.1021/acs.est.6b02216.

Richardson, A.K., Chadha, M., Rapp-Wright, H., Mills, G.A., Fones, G.R., Gravell, A., Stürzenbaum, S., Cowan, D.A., Neep, D.J., Barron, L.P., 2021. Rapid direct analysis of river water and machine learning assisted suspect screening of emerging contaminants in passive sampler extracts. Anal. Methods https://doi.org/10.1039/d0ay02013c.

Roll, I.B., Halden, R.U., 2016. Critical review of factors governing data quality of integrative samplers employed in environmental water monitoring. Water Res., 200–207 https://doi.org/10.1016/j.watres.2016.02.048 Pergamon May 1.

Rúa-Gómez, P.C., Guedez, A.A., Ania, C.O., Püttmann, W., 2012. Upgrading of Wastewater Treatment Plants Through the Use of Unconventional Treatment Technologies: Removal of Lidocaine, Tramadol, Venlafaxine and Their Metabolites. 4, pp. 650–669. https://doi.org/10.3390/w4030650.

Salim, F., Górecki, T., 2019. Theory and modelling approaches to passive sampling. Environ Sci Process Impacts 21 (10), 1618–1641. https://doi.org/10.1039/c9em00215d.

Schnell, S., Bawa-Allah, K., Otitoloju, A., Hogstrand, C., Miller, T.H., Barron, L.P., Bury, N.R., 2015. Environmental monitoring of urban streams using a primary fish gill cell culture system (FIGCS). Ecotoxicol. Environ. Saf. 120, 279–285. https://doi.org/10.1016/J.ECOENV.2015.06.012.

Schreiner, V.C., Bakanov, N., Kattwinkel, M., Könemann, S., Kunz, S., Vermeirssen, E.L.M., Schäfer, R.B., 2020. Sampling rates for passive samplers exposed to a field-relevant peak of 42 organic pesticides. Sci. Total Environ. 740, 140376. https://doi.org/10.1016/j.scitotenv.2020.140376.

Shaw, M., Eaglesham, G., Mueller, J.F., 2009. Uptake and release of polar compounds in SDB-RPS EmporeTM disks; implications for their use as passive samplers. Chemosphere 75 (1), 1–7. https://doi.org/10.1016/j.chemosphere.2008.11.072.

Taylor, A.C., Fones, G.R., Vrana, B., Mills, G.A., 2019. Applications for passive sampling of hydrophobic organic contaminants in water—a review. Crit. Rev. Anal. Chem., 1–35 https://doi.org/10.1080/10408347.2019.1675043.

Taylor, A.C., Fones, G.R., Mills, G.A., 2020. Trends in the use of Passive sampling for monitoring polar pesticides in water. Trends Environ. Anal. Chem., e00096 https://doi.org/10.1016/j.teac.2020.e00096 Elsevier BV May 1.

Townsend, I., Jones, L., Broom, M., Gravell, A., Schumacher, M., Fones, G.R., Greenwood, R., Mills, G.A., 2018. Calibration and application of the Chemcatcher® passive sampler for monitoring acidic herbicides in the River Exe, UK Catchment. Environ. Sci. Pollut. Res. 25 (25), 25130–25142. https://doi.org/10.1007/s11356-018-2556-3.

UK Centre for Ecology & Hydrology. UK water resources portal. https://eip.ceh.ac.uk/hydrology/water-resources/#introText. (Accessed 14 July 2021).

US Enviromental Protection Agency. Contaminant candidate list 4 https://www.federalregister.gov/documents/2016/11/17/2016-27667/drinking-water-contaminant-candidate-list-4-final (accessed Jun 16, 2021).

Vermeirssen, E.L.M., Bramaz, N., Hollender, J., Singer, H., Escher, B.I., 2009. Passive sampling combined with ecotoxicological and chemical analysis of pharmaceuticals and biocides - evaluation of three ChemcatcherTM configurations. Water Res. 43 (4), 903–914. https://doi.org/10.1016/j.watres.2008.11.026.

Vermeirssen, E.L.M., Dietschweiler, C., Escher, B.I., Van Der Voet, J., Hollender, J., 2012. Transfer kinetics of polar organic compounds over polyethersulfone membranes in the passive samplers Pocis and chemcatcher. Environ. Sci. Technol. 46 (12), 6759–6766. https://doi.org/10.1021/es3007854.

Vermeirssen, E.L.M., Dietschweiler, C., Escher, B.I., Van Der Voet, J., Hollender, J., 2013. Uptake and release kinetics of 22 polar organic Chemicals in the Chemcatcher Passive Sampler. Anal. Bioanal. Chem. 405 (15), 5225–5236. https://doi.org/10.1007/s00216-013-6878-1.

Villegas, M., Cetinic, Z., Shakeri, A., Didar, T.F., 2018. Fabricating smooth PDMS microfluidic channels from low-resolution 3D printed molds using an omniphobic lubricant-infused coating. Anal. Chim. Acta 1000, 248–255. https://doi.org/10.1016/j.aca.2017.11.063.

Vrana, B., Allan, I.J., Greenwood, R., Mills, G.A., Dominiak, E., Svensson, K., Knutsson, J., Morrison, G., 2005. Passive sampling techniques for monitoring pollutants in water. TrAC - Trends Anal. Chem. 24 (10), 845–868. https://doi.org/10.1016/j.trac.2005.06.006.

Vrana, B, Mills, G.A., Dominiak, E., Greenwood, R., 2006. Calibration of the chemcatcher passive sampler for the monitoring of priority organic pollutants in water. Environ. Pollut. 142 (2), 333–343. https://doi.org/10.1016/j.envpol.2005.10.033.

Vrana, B, Mills, G.A., Kotterman, M., Leonards, P., Booij, K., Greenwood, R., 2007. Modelling and field application of the chemcatcher passive sampler calibration data for the monitoring of hydrophobic organic pollutants in water. Environ. Pollut. 145 (3), 895–904. https://doi.org/10.1016/j.envpol.2006.04.030.

Vrana, B, Urík, J., Fedorova, G., Švecová, H., Grabicová, K., Golovko, O., Randák, T., Grabic, R., 2021. In situ calibration of polar organic chemical integrative sampler (POCIS) for monitoring of pharmaceuticals in surface waters. Environ. Pollut. 269, 116121. https://doi.org/10.1016/j.envpol.2020.116121.

Wang, Z., Walker, G.W., Muir, D.C.G., Nagatani-Yoshida, K., 2020. Toward a global understanding of chemical pollution: a first comprehensive analysis of national and regional chemical inventories. Environ. Sci. Technol. 54, 2575–2584. https://doi.org/10.1021/ACS.EST.9B06379/SUPPL_FILE/ES9B06379_SI_001.PDF.

Wang, J.X., Cheng, Y.F., Pan, X.H., Luo, P., 2022. Tissue-specific accumulation, transformation, and depuration of fipronil in adult crucian carp (Carassius Auratus). Ecotoxicol. Environ. Saf. 232, 113234. https://doi.org/10.1016/J.ECOENV.2022.113234.

Wilkinson, J.L., Hooda, P.S., Swinden, J., Barker, J., Barton, S., 2018. Spatial (Bio)Accumulation of pharmaceuticals, illicit drugs, plasticisers, perfluorinated compounds and metabolites in river sediment, Aquatic plants and benthic organisms. Environ. Pollut. 234, 864–875. https://doi.org/10.1016/j.envpol.2017.11.090.

Wilkinson, J.L., Boxall, A.B.A., Kolpin, D.W., Leung, K.M.Y., Lai, R.W.S., Galban-Malag, C., Adell, A.D., Mondon, J., Metian, M., Marchant, R.A., Bouzas-Monroy, A., Cuni-Sanchez, A., Coors, A., Carriquiriborde, P., Rojo, M., Gordon, C., Cara, M., Moermond, M., Luarte, T., Petrosyan, V., Perikhanyan, Y., Mahon, C.S., McGurk, C.J., Hofmann, T., Kormoker, T., Iniguez, V., Guzman-Otazo, J., Tavares, J.L., de Figueiredo, F.G., Razzolini, M.T.P., Dougnon, V., Gbaguidi, G., Traore, O., Blais, J.M., Kimpe, L.E., Wong, M., Wong, D., Ntchantcho, R., Pizarro, J., Ying, G.G., Chen, C.E., Paez, M., Martınez-Lara, J., Otamonga, J.P., Pote, J., Ifo, S.A., Wilson, P., Echeverrıa-Saenz, S., Udikovic-Kolic, N., Milakovic, M., Fatta-Kassinos, D., Ioannou-Ttofa, L., Belusova, V., Vymazal, J., Cardenas-Bustamante, M., Kassa, B.A., Garric, J., Chaumot, A., Gibba, P., Kunchulia, I., Seidensticker, S., Lyberatos, G., Halldorsson, H.P., Melling, M., Shashidhar, T., Lamba, M., Nastiti, A., Supriatin, A., Pourang, N., Abedini, A., Abdullah, O., Gharbia, S.S., Pilla, F., Chefetz, B., Topaz, T., Yao, K.M., Aubakirova, B., Beisenova, R., Olaka, L., Mulu, J.K., Chatanga, P., Ntuli, V., Blama, N.T., Sherif, S., Aris, A.Z., Looi, L.J., Niang, M., Traore, S.T., Oldenkamp, R., Ogunbanwo, O., Ashfaq, M., Iqbal, M., Abdeen, Z., O'Dea, A., Morales-Saldaña, J.M., Custodio, M., de la Cruz, H., Navarrete, I., Carvalho, F., Gogra, A.B., Koroma, B.M., Cerkvenik-Flajs, V., Gombac, M., Thwala, M., Choi, K., Kang, H., Celestino Ladu, J.L., Rico, A., Amerasinghe, P., Sobek, A., Horlitz, G., Zenker, A.K., King, A.C., Jiang, J.J., Kariuki, R., Tumbo, M., Tezel, U., Onay, T.T., Lejju, J.B., Vystavna, Y., Vergeles, Y., Heinzen, H., Perez-Parada, A., Sims, D.B., Figy, M., Good, D., Teta, C., 2022. Pharmaceutical pollution of the world's rivers. Proc. Natl. Acad. Sci. U. S. A. 119 (8). https://doi.org/10.1073/PNAS.2113947119/SUPPL_FILE/PNAS.2113947119.SD12.XLSX.

Yuen, P.K., 2008. SmartBuild - a truly plug-n-play modular microfluidic system. Lab Chip 8 (8), 1374–1378. https://doi.org/10.1039/b805086d.

Yuen, P.K., 2016. A reconfigurable stick-n-play modular microfluidic system using magnetic interconnects. Lab Chip 16 (19), 3700–3707. https://doi.org/10.1039/c6lc00741d.

Zenker, A., Cicero, M.R., Prestinaci, F., Bottoni, P., Carere, M., 2014. Bioaccumulation and biomagnification potential of pharmaceuticals with a focus to the Aquatic environment. J. Environ. Manag. 378–387 https://doi.org/10.1016/j.jenvman.2013.12.017 Academic Press January 15.

Water_quality_monitoring_data_GCMS_LCMS_Semiquantitative. https://environment.data.gov.uk/portalstg/home/item.html?id=b76f059c3f294678840a2590f61f7e59. (Accessed 17 September 2021).